Chapter 6

Synthesis of carbon-silica nanocomposites from algae

In this chapter, synthesis of carbon-silica nanocomposites from algal biomass by pyrolysis at relatively lower temperature was discussed. A total of three algae (*Scytonema guyanense, Trentepohlia aurea, Spirogyra neglecta*) were used as precursors for the production of carbon-silica nanocomposites. Antioxidant efficacy of the synthesised nanocomposites was monitored using DPPH as free radical source.

6.1. Introduction

Carbon and silicon, the most abundant elements on earth play an important role in materials science due to their importance in both practical applications and academic research [1]. In order to synergistically utilize their interesting properties, different preparative pathways for carbon/silica hybrid nanocomposites are being explored [2]. Use of dried biomass, aqueous or organic extract of plants including lower forms such as fungi, algae and lichens for accessing metal based nanoparticles has drawn wide interest of researchers in the last decade or so [3-6]. Pyrolysis of plant based precursors to afford carbon nanomaterials, however, are only recently beginning to find sporadic attention [7]. Besides carbon nanomaterials, interests in carbon

nanocomposite are rapidly growing[8, 9]. Strongly coupled hybrids of inorganic nanomaterials and novel graphitic nano-carbon materials such as carbon nanotubes and graphene represent a heuristic approach to synthesize electrochemical energy storage materials. Inorganic-nano carbon hybrid materials have captured fascinating interests as high performance electrode materials than traditional counterparts made by simple physical mixing of electrochemically active inorganic element and conducting carbon materials. Nano-carbon with various degrees of oxidation provides a novel substrate for nanoparticle nucleation and growth [10].While graphene, CNT, CNF materials have recently earned a lot of attention as a viable alternative to replace activated carbon materials, the synthesis protocols are quite expensive. Due to large specific capacity and low working potential, silicon is considered as a suitable candidate to substitute existing graphitic anodes. Electrodes made of pure silicon, however, have shown poor mechanical integrity and dramatic expansion of the material during battery operation thus precluding their adoption [11]. The carbon-silicon nanocomposites, on the other hand, provide excellent mechanical, electrochemical, and electrical properties of carbon with the superior lithium intercalation ability of silicon. The manufacture of carbon-silicon composites for anodes by mechanical milling has been explored [12]. A new class of silica-carbon nanocomposite has recently been employed as solid catalyst for cellulose hydrolysis that yielded high glucose compared to reference catalysts and commercial zeolites [13]. It is believed that the organic part of the composite material offers flexibility and versatility for further functionalization while the silica component renders mechanical and thermal stability. To ensure high entanglement of carbon and silica in the nanocomposite, an evaporation-induced triconstituent co-assembly method had been explored [14]. Besides nanoparticle size and composition, particle shape also plays a crucial role in achieving different applications. Several chemical routes which were explored to prepare carbon-silica hybrid materials from different carbon and silicon based precursors are complicated, often expensive, and based on toxic carbon or silicon source [15, 16]. Rice husk has been extensively worked upon to afford carbon-silicon material. Reviews by Lee and Cutler [17] and a very recent one by Chiew and Cheong [18] dealt with carbon-silicon material from plant based biomass. Though synthesis of C-Si composite material from biomass is marred with problems of low yield and impurities, the renewable and abundant plant biomass provide a viable option for consideration. The cellulosic component in these plant-based biomasses

can be readily converted to carbon with lot of silica getting accumulated at the outer epidermis [19]. This leads to intimate contact between carbon content and silica generating high surface area by the nanoparticle [20, 21]. In this chapter we report a cheap, renewable and scalable green protocol for accessing carbon-silica hybrid nanomaterial from inexpensive algal biomass such as *Scytonema guyanense, Trentepohlia aurea, Spirogyra neglecta*.

6.2. Carbon- silica nanocomposites from a blue-green alga, *Scytonema guyanense*

6.2.1.Materials

The alga was collected from the exposed surfaces (concrete substratum) of the departmental building in Assam University campus, located near Silchar town (Assam), India. Based on morphological characteristics, the species has been identified following standard keys to be *Scytonema guyanense* var. *minus*, a blue green alga (**Fig.6.1**)[22]. It is found to grow luxuriantly on stony surfaces forming thick mats during the rainy season. The sample was thoroughly washed with distilled water to remove any dirt, shade dried, ground to powder in a glass mortar and used as such.

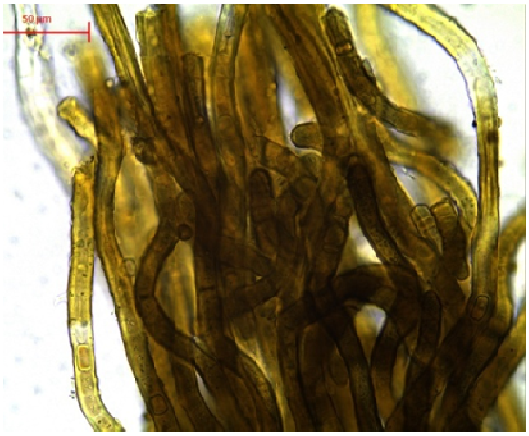

Fig.6.1. Optical microscopic image of *Scytonema guyanense* var. *minus*

6.2.2. Synthesisof nanocomposites

The production of carbon-silica nanocomposite from algal (*Scytonemasp*.) biomass was carried out by pyrolysis under inert condition. The dried algal biomass (10g) taken in a quartz tube was heated to 600^0C in a chemical vapour deposition furnace at a rate of 7^0C /min for 2 hours under argon flow rate of $6cm^3$/min to afford a black powder. The yield recorded was 2.8 g, (~30%).

6.2.3. Results and discussion

The algal biomass afforded the carbon-silica nanocomposite in relatively good yield considering that most of the algal biomass volatilized off at the experimental temperature. The synthesis is carried out using the algal biomass as precursor simply by direct pyrolysis under inert atmosphere and no other reagents were used for pretreatments. At a temperature below ~600^0C or so and holding time less than 2 hour, the pyrolysis was found to be incomplete as the material obtained was agglomerated with lot of extraneous matter. Organic compounds in plant biomass tend to decompose at ~400^0C and cellulose decomposition and the cleavage of bonds of organic molecules to silicon usually takes place at ~550^0C [23]. A higher temperature (upto 700^0C) and holding time of pyrolysis (upto 4 hours) did not appreciably alter the morphology or yield of the material. Thus the temperature of 600^0C and a holding time of 2 hour were set as optimum condition to gain access to the nanocomposite. It is pertinent to mention herein that besides such carbonization methods, multicomponent co-assembly process have also recently beginning to attract fancy of researchers to afford carbon-silica nanocomposite [24, 25]. The chemical reaction involved in the present pyrolytic process may be represented by

$$\text{Algal biomass} \xrightarrow{\triangle} \text{CO + volatile organics + ash}$$

The ash residue is the carbonized silica. In oxidative treatment, a similar pathway is believed to be involved with CO_2 being a additional product [26].The filamentous alga, *Scytonema sp.* used herein has been a source of homogeneous chemical raw material for the production of carbon-silica nanocomposite.

6.2.3.1. Scanning electron microscopy and transmission electron microscopy

The algal biomass afforded the carbon-silica nanocomposite in relatively good yield. The SEM micrograph showed a flake type morphology with spherical particles embedded (**Fig.6.2**).

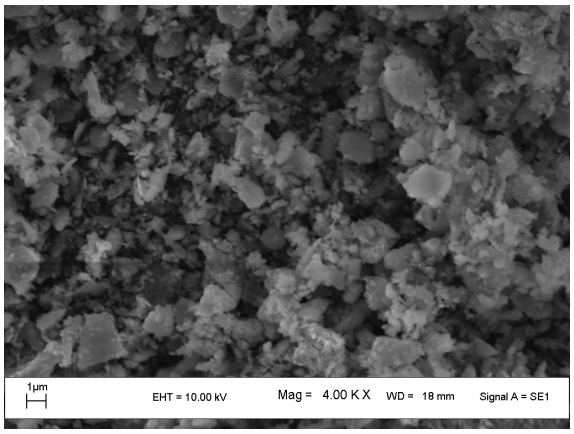

Fig.6.2.SEM micrograph of nanocompositefrom blue-green alga

The TEM micrographs of nanocomposites (**Fig.6.3**) revealed the presence of silica nanoparticles of non-uniform sizes embedded in carbon nanoflakes. The thicknesses of the flakes are ~3 nm. The HRTEM micrographs showed silica nanoparticles to be quasi-spherical five-fold multiply twinned. The 0.18 nm inter-planar distance of lattice fringes correspond to $11\bar{2}$ plane of silica.

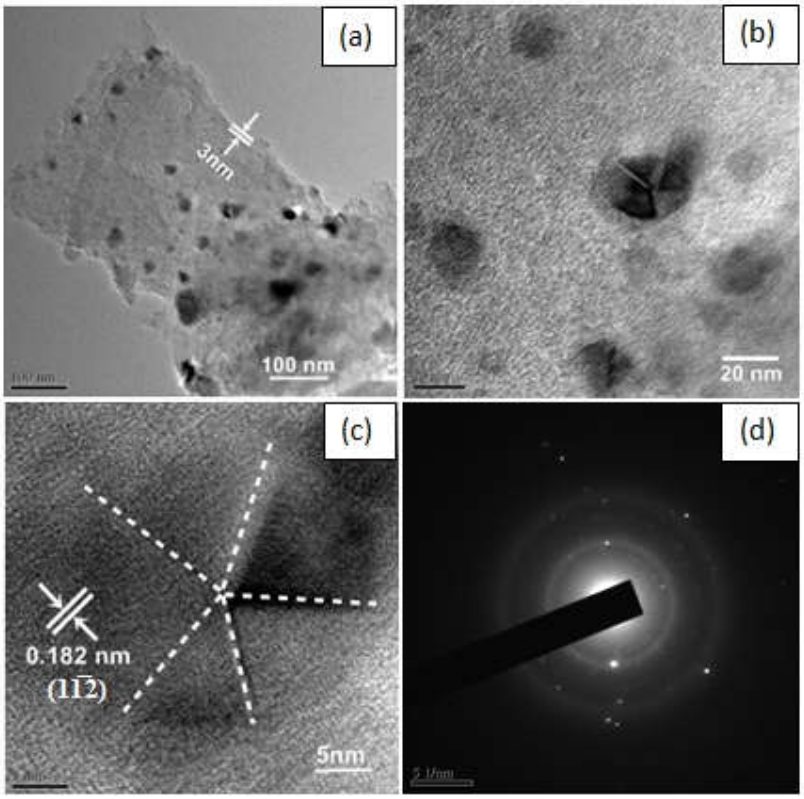

Fig.6.3.(a,b) TEM image **(c)** HRTEM image and **(d)**SAED pattern of nanocompositesfrom blue-green alga

Circular rings typical of graphitic carbon and scattered spots originating from embedded silica nanoparticles are both visible in the SAED profile (**Fig.6.3(d)**). The size of the embedded silica nanoparticles as revealed from HRTEM ranged from 25-40 nm.

6.2.3.2. Energy dispersive spectral (EDS) study

The EDS analysis (**Fig.6.4**) revealed the occurrence of carbon, silicon and oxygen as the major constituents with minor contributions from aluminium.

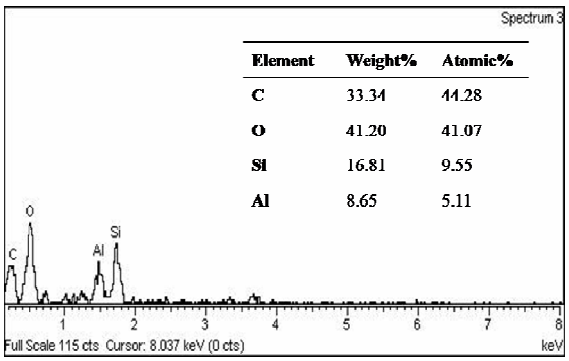

Fig.6.4.EDS and elemental composition of nanocompositesfromblue-green alga

6.2.3.3.FT-IR study

The FT-IR spectrum (**Fig.6.5**) exhibited diagnostic features at 720 cm^{-1} for the vibrational mode ($\nu_{Si\text{-}O\text{-}Si} + \rho_{CH2}$), 790 cm^{-1} for the combination band ($\nu_{Si\text{-}C} + \rho_{a(CH3)}$) and at 1080 cm^{-1} attributable to (ν_s Si-O-Si) [27]. A relatively strong band at 1430 cm^{-1} is presumed to be associated with CH_2 deformation mode of graphitic carbon matrix. A rather weak and broad band at 3650 cm^{-1} was assigned to –OH function which may be attributed to surface adsorbed water [28].

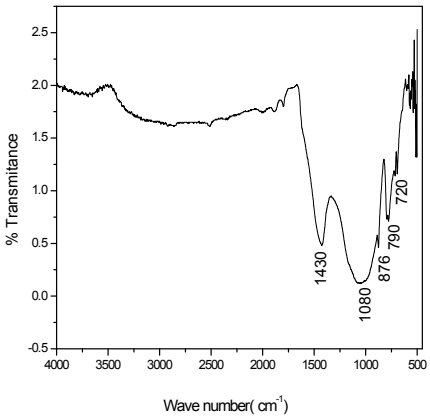

Fig.6.5.FT-IR spectrum of nanocomposites from blue-green alga

6.2.3.4.Powder X-ray diffraction study

The powder X-ray diffraction study was carried out for identification of phases exhibited by the synthesised nanocomposites.The X-ray diffraction pattern (**Fig.6.6**) was replete with rather large number of peaks (2θ ~ 10° to 80°), some correspond to the crystallographic planes of hexagonal silicon dioxide (JCPDS file no.85-0504) while others relate to hexagonal graphitic carbon (JCPDS file no.23-0064). The diffraction peaks were sharp indicating large crystallite size. The average crystallite size (~41nm) obtained using a Gaussian fit following Debye-Scherrer method is compatible with that obtained from TEM study.

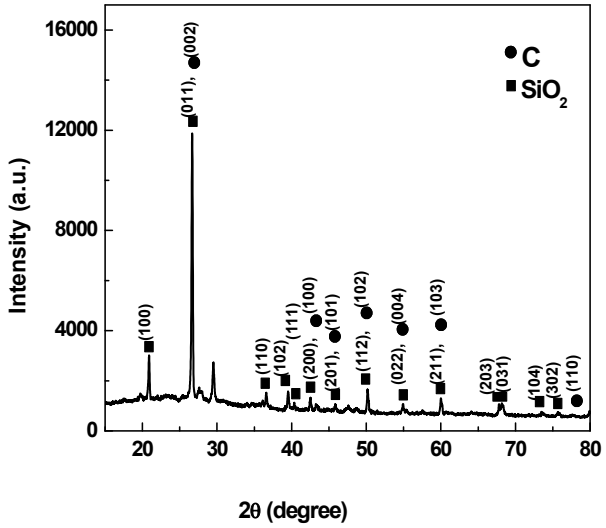

Fig.6.6. Powder X-Ray diffraction pattern of nanocompositesfrom blue-green alga

6.2.3.5.Fluorescent study

The material is fluorescent showing a broad emission at 340 nm at an excitation wavelength 240 nm. It is pertinent to mention, that a lot of interests exist in the fluorescence property of nontoxic, biocompatible carbon-silica nanocomposites that are of relevance to bio-imaging and bio-analytical applications [29,30]. Though some reports on CNT-nano-silica are documented, photoluminescence properties of carbon-silica nanocomposite have not received much attention till date [31].

6.2.3.6. Antioxidant activity of nanocomposite

The antioxidant activity of the nanocomposite was assessed using a modified DPPH methodfor insoluble solids[32]by UV-visible spectroscopy noting the colour change from purple to yellowas described in detail in the section **3.4.3.5** of Chapter 3.The DPPH scavenging percentage were calculated from decline in absorbance at 517 nm, which corresponds to the quantity of DPPH in methanolic solution. It is evident from the **Fig.6.7(a)** that after 60 minutes more than50% of the DPPH got scavenged for 15 mg of the nanocomposites. The SC-50 value was ascertained graphically (**Fig.6.7(b)**) and was foundto be 13.5 mg. It may be mentioned that the free radical scavenging capacity of nanosilica-gallic acid as nanoantioxidant is also well recognised[33, 34].

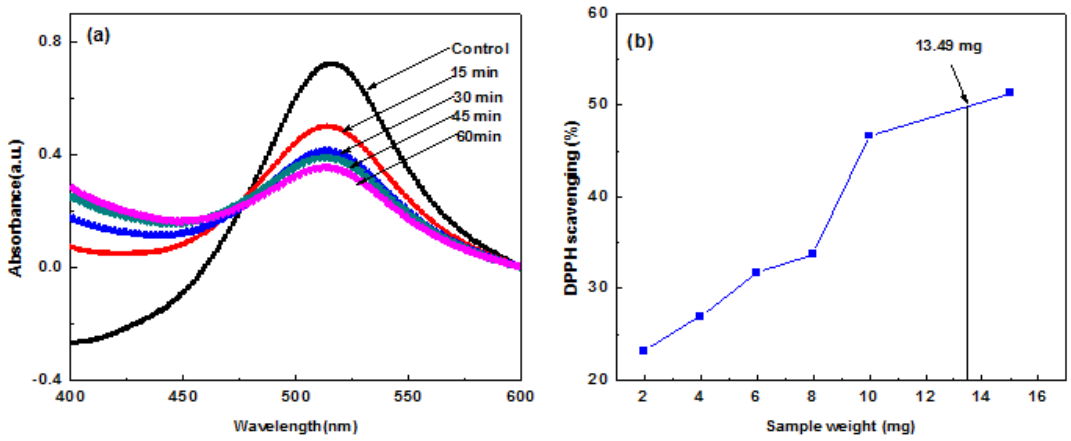

Fig.6.7 (a) Time dependent DPPH scavenging and **(b)** DPPH scavenging (%) at different weight of nanocomposites

6.3. Carbon- silica nanocomposites from a green alga, *Trentepohlia aurea*

6.3.1. Materials

The green filamentous alga, *Trentepohlia aurea*, (**Fig.6.8**) wascollected from bark of betel nut tree (*Areca catechu*) growing in Cachar district of the state of Assam, India. The biomass was thoroughly washed with deionised water to remove any dirt, shade dried and used as a precursor for the production of nanocomposite. Rich carotene content imparts a deep orange colour to the alga[35].

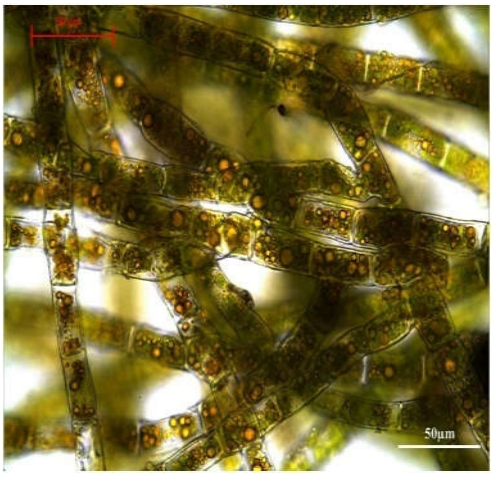

Fig.6.8. Optical microscopic image of *Trentepohlia aurea*

6.3.2. Synthesisof nanocomposites

Carbon-silica nanocomposites were produced from the algal biomass (*Trentepohlia* sp.) by pyrolysis in a CVD furnace. A quartz boat loaded with the algal biomass (10 g) inserted in a horizontal quartz tube is placed in the furnace. The tube was initially flushed with argon gas to eliminate air from the tube. The gas was then purged at a flow rate of 6cm^3/min. The furnace was heated to 600^{0}C at a rate of 7^{0}C/ min for 2 hour to complete the process of pyrolysis. The system was then allowed to cool to room temperature under inert condition and the black nanocomposite materials was taken out from the quartz boat and analyzed as obtained (yield 2.6 g).

6.3.3. Results and discussion

Pyrolysis of the algalbiomas*s (Trentepohlia sp.)* at 600^{0}C afforded the carbon-silica nanocomposites in ~25% yield by weight of precursor biomass. The hybrid carbon-silica nanomaterial can be readily brought into dispersion by ultrasonication in aqueous and common organic solvent media (ethanol and methanol). The rich carotenoid content of the alga led us to presume this to be a suitable precursor for carbon nanomaterials.

6.3.3.1. Transmission electron microscopy

The TEM micrographs (**Fig.6.9**) revealed spherical silica nanoparticles of diameter ~20 nm embedded in carbon nanoflakes. The HRTEM micrograph**(Fig.6.9(b))** showed that thicknesses of the flakes are ~1.5 nm. The 0.33 nm inter-planar distance

of lattice fringes correspond to (002) plane of graphitic carbon. Both smooth concentric rings typical of stacked graphitic carbon layers and scattered spots originating from embedded silica nanoparticles are visible in the selected areaelectron diffraction (SAED) profile**(Fig.6.9(c,d))**. The black spherical spots observed in the TEM are typical of silica crystallite.

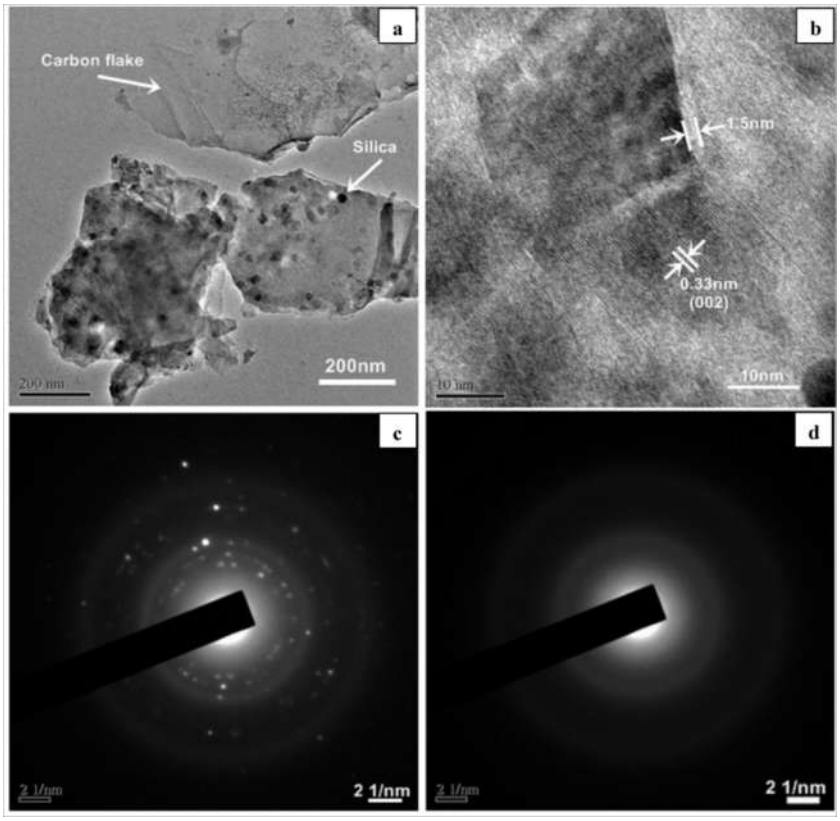

Fig.6.9.(a) TEM image **(b)** HRTEM image and**(c,d)** SAED pattern of nanocomposite from *Trentepohlia aurea*

6.3.3.2. Powder X-Ray diffraction study

The XRD pattern**(Fig.6.10)**exhibited a number of intense and sharp peaks assigned to Bragg reflections from both graphitic carbon and silicon dioxide crystal. The X-ray diffraction pattern showed peaks (20.87°, 26.60°, 36.56°, 39.51°,40.31°, 42.45°, 45.77°, 50.14°, 54.86°, 59.96°, 64.00°, 67.74°, 68.07°, 73.48°, 75.70° and 77.62°) of 2θ values ranging from 10° to 80°, which correspond to the (100), (011), (110), (102), (111), (200), (201), (112), (022), (211), (113), (203), (031), (104), (302) and (220) crystallographic planes of hexagonal silicon dioxide (JCPDS file no.85-0504) and peaks (26.60°, 42.45°, 45.77°, 50.14°, 54.86°, 59.96° and 77.62°) of 2θ values also

correspond to the (002), (100), (101), (102),(004), (103) and (110) crystallographic planes of hexagonal graphitic carbon (JCPDS file no. 23-0064).The average crystallite size (~20nm) obtained using a Gaussian fit following Debye-Scherrer method is compatible with that obtained from TEM study.

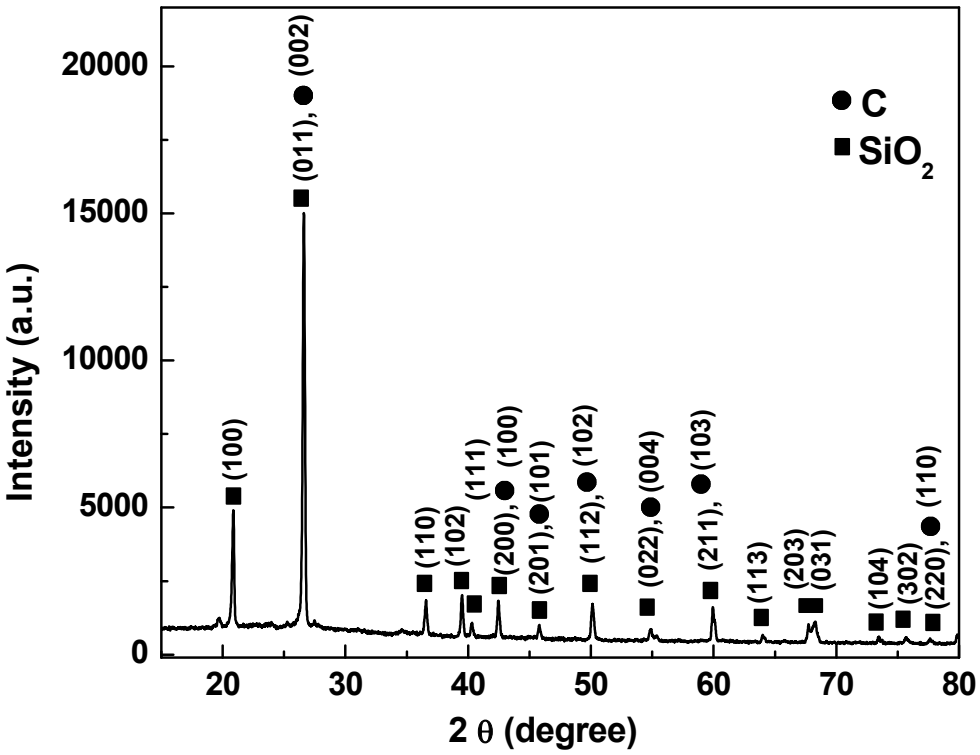

Fig.6.10. Powder X-ray diffraction of nanocompositesfrom *Trentepohlia aurea*

6.3.3.3. FT-IR study

The FT-IR spectrum (**Fig.6.11**) exhibited diagnostic features at 780 cm^{-1} for the combination band ($\nu_{Si-C} + \rho_{a\ (CH3)}$) and at 1080 cm^{-1} attributable silica (ν_s Si-O-Si) [27]. The band at 485 cm^{-1} belongs to bending vibration of O-Si-O [36]. A rather weak and broad band at 3650 $cm^{-1}$was assigned to –OH function which may be attributed to surface adsorbed water [28].

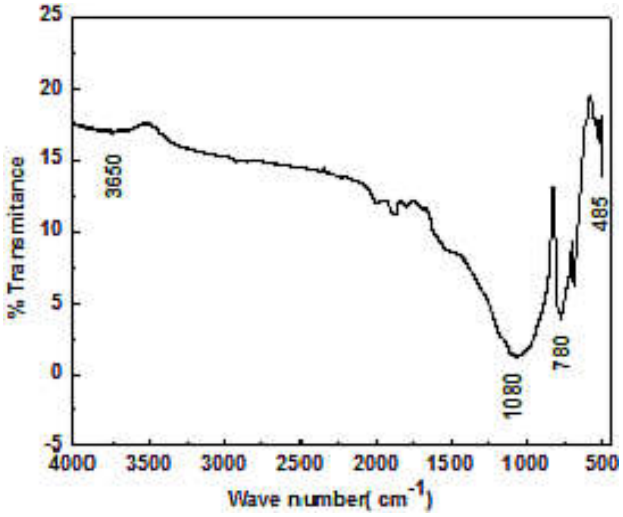

Fig.6.11.FT-IR spectrum of nanocomposites from *Trentepohlia aurea*

6.3.3.4. Antioxidant activity of nanocomposite

The antioxidant activity of the nanocomposite was studied *in vitro* using a modified DPPH method for insoluble solids [32] by UV-visible spectroscopy noting the colour change from purple to yellow. The nanocomposite with DPPH added, showed a decline in absorbance at 517 nm **(Fig.6.12 (a))**. About 50% of DPPH was scavenged after one hour for 20 mg of the material with SC-50 value ascertained to be 19.8 mg **(Fig.6.12(b)).**

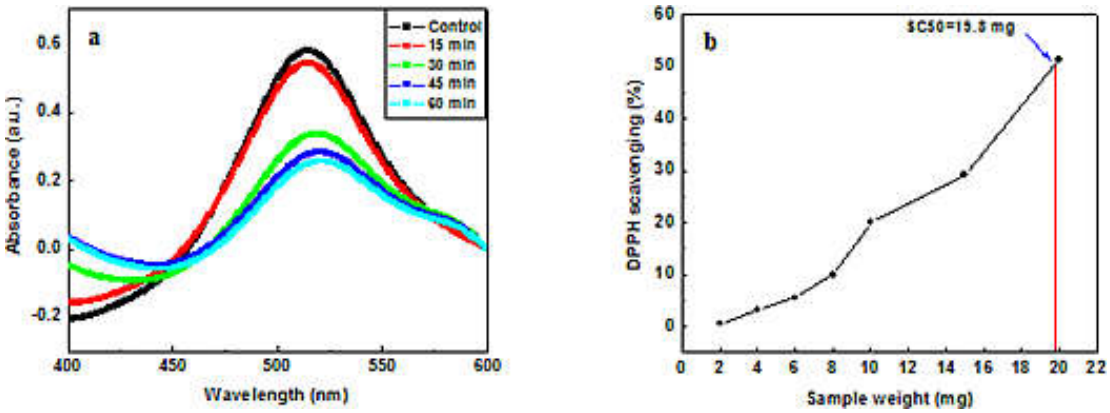

Fig.6.12.(a) Time dependent DPPH scavenging and **(b)** DPPH scavenging (%) at different weight of nanocomposites

6.4. Carbon- silica nanocomposites from a green alga, *spirogyra* sp.

6.4.1. Materials

The alga was collected from pond ecosystem in Silchar (Assam), India. Based on morphological characteristics, the species has been identified following standard keys to be *Spirogyra neglecta* (Hassall) Kuetzing, a green alga(**Fig.6.13**)[22]. The sample was thoroughly washed with distilled water to remove any dirt, shade dried, ground to powder in a glass mortar and used as such.

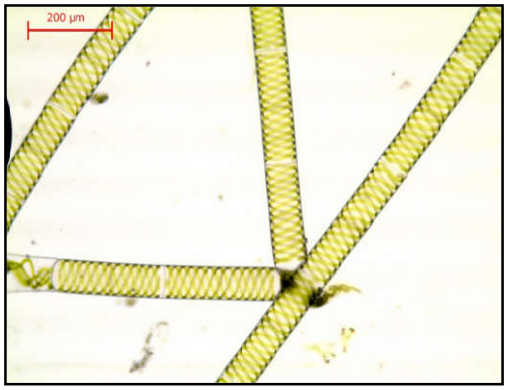

Fig.6.13. Optical microscopic image of *Spirogyra neglecta*

6.4.2. Synthesisof nanocomposites

Carbon-silica nanocomposites were produced from the algal biomass (*Spirogyra sp*.) by pyrolysis in a CVD furnace. A quartz boat loaded with the algal biomass (10 g) inserted in a horizontal quartz tube is placed in the furnace. The tube was initially flushed with argon gas to eliminate air from the tube. The gas was then purged at a flow rate of 6cm^3/min. The furnace was heated to 600 ^{0}C at a rate of 7 ^{0}C min for 2 hours to complete the process of pyrolysis. The system was then allowed to cool to room temperature under inert condition and the black nanocomposite materials was collected from the quartz boat and analyzed as obtained(yield 2.1 g).

6.4.3. Results and discussion

The algal biomass afforded the carbon-silica nanocomposite in relatively good yield(~20%). The hybrid C-SiO_2 material can be readily brought into dispersion by ultrasonication in aqueous and common organic solvent media (ethanol and methanol).

6.4.3.1. Transmission electron microscopy

The TEM micrograph (**Fig.6.14**) revealedspherical silica nanoparticles of diameter ~5nm embedded in ~4nm thick carbon nanoflakes**(Fig.6.14 (a, inset)**. The HRTEM micrographs showed silica nanoparticles to be almost spherical. The 0.33 nm inter-planar distance of lattice fringes correspond to 002 plane of graphitic carbon.The black spherical spots observed in the TEM are typical of silica crystallite. The diffused circular rings in the SAED pattern in **Fig. 6.14(c)** are identified as reflections from the graphitic ordering of the carbon component while the regular characteristic dot pattern**(Fig.6.14(d))**are ascribed to embedded silica of the composite.

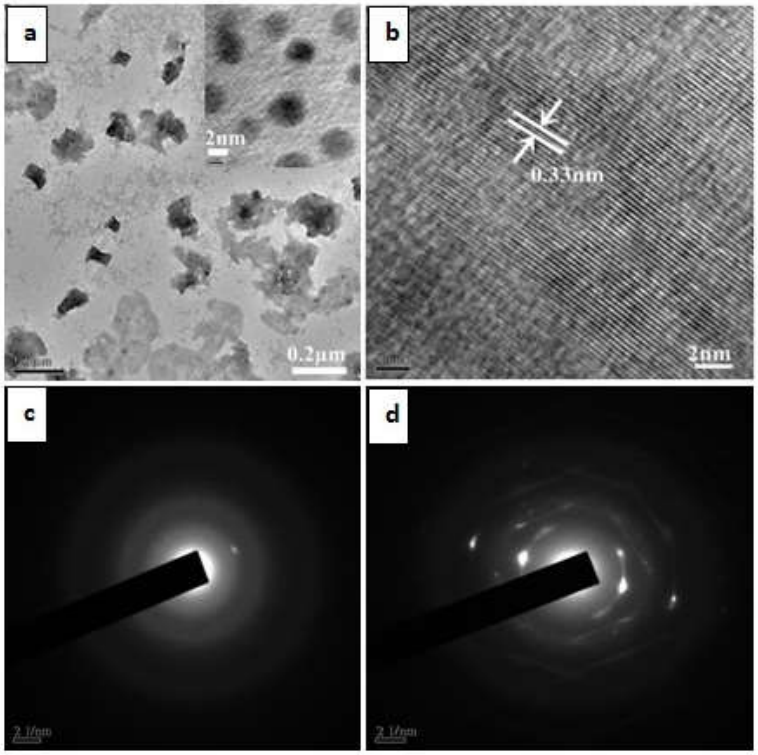

Fig.6.14.(a)TEM image **(b)** HRTEM image and **(c, d)** SAED pattern of nanocomposite obtained from a green alga

6.4.3.2. Powder X-Ray diffraction study

The XRD pattern**(Fig.6.15)**exhibited a number of intense and sharp peaks assigned toBragg reflections from both graphitic carbon and silicon dioxide crystal. The X-ray diffraction pattern showed peaks (20.87°, 36.56°, 39.51°,40.31°, 42.45°, 45.77°, 50.14°, 54.86°, 59.96°, 64.00° and 67.74°) of 2θ values ranging from 10° to 80°, which correspond to the (100), (110), (102), (111), (200), (201), (112), (022), (211),

(113) and (203) crystallographic planes of hexagonal silicon dioxide (JCPDS file no.85-0504) and peaks (26.60°, 42.45°, 45.77°, 50.14°, 54.86° and 59.96°) of 2θ values also correspond to the (002), (100), (101), (102),(004) and (103) crystallographic planes of hexagonal graphitic carbon (JCPDS file no. 23-0064). The average crystallite size is calculated to be 8 nm using the Debye-Scherrer's method for 100 plane of silica.

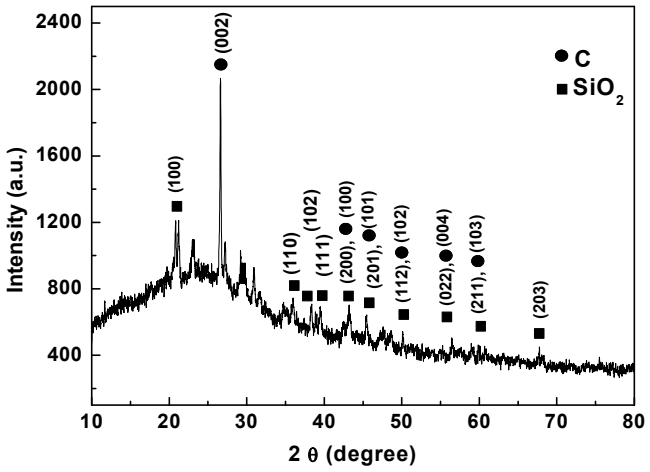

Fig.6.15. Powder X-Ray diffraction of nanocomposites from green alga

6.4.3.3. FT-IR study

The FT-IR spectrum (**Fig.6.16**) exhibited diagnostic features at 485 cm^{-1} for the bending vibrational mode O-Si-O, at 780 cm^{-1} for the combination band (ν_{Si-C} + $\rho_{a(CH3)}$) and at 1070 cm^{-1} attributable to silica (υ_s Si-O-Si) [27, 35]. A relatively intense band at 1430 cm^{-1} is due to stretching vibration of conjugated -C=C-of graphitic carbon matrix. A rather weak and broad band at 3650 cm^{-1} was assigned to–OH function which may be attributed to surface adsorbed water [28].

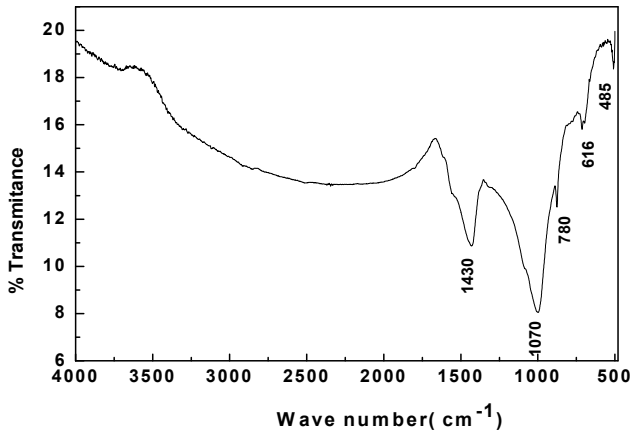

Fig.6.16. FT-IR spectrum of nanocomposites obtained from a green alga

6.4.3.4. Antioxidant activity

The synthesised carbon-silica nanocompositefrom *Spirogyra sp.* didn't show any significant antioxidant property although the composite from *Scytonema*sp.and *Trentepohlia sp.* were found to be highly effective against DPPH**(Table 6.1)**. The behaviour may be corelated to average crysallilte size of the embedded silica nanoparticles in the carbonnanoflakes. It was observed that the larger the crystallite size of silica higher is the efficacy of the material towards the free radical scavenging. It is pertinent here to mention that the antioxidant profile of CNT followed a reverse order (Section **3.4.3.5,** Chapter3).

Table6.1 Antioxidant efficacy of nanocomposites

Nanocomposite	Average crystallite size	SC-50
From *Scytonema sp.*	41 nm	13.5 mg
From *Trentepohlia sp.*	20 nm	19.8 mg
From *Spirogyra sp.*	8 nm	----

References

[1] Peng, H., Zhu, Y., Peterson, D. E., & Lu, Y. *Adv. Mater.*, 2008, **20**, 1199.

[2] Camargo, P. H. C., Satyanarayana, K. G., & Wypych, F. *Mat. Res.*, 2009, **12**, 1.

[3] FarooqaAdil, S., & Rafiq H aSiddiqui, M. *Dalton Trans.,* 2015, **44**, 9709.

[4] Sharma, B., Purkayastha, D. D., Hazra, S., Gogoi, L., Bhattacharjee, C. R., Ghosh, N. N., & Rout, J. *Mater. Lett.*, 2014, **116**, 94.

[5] Duran, N., Marcato, P. D., Duran, M., Yadav, A., Gade, A., & Rai, M. *Appl. Microbiol. Biotechnol.,* 2011, **90**, 1609.

[6] Iravani, S.*Green Chem*., 2011, **13**, 2638.

[7] Shen, Y., Zhao, P., & Shao, Q. *Micropor. Mesopor. Mat.*, 2014, **188**, 46.

[8] Li, X., Zhang, G., Zhang, L., Zhong, M., & Yuan, X. *Int. J. Electrochem. Sci.*, 2015, **10**, 2802.

[9] Ghosh, P., Afre, R. A., Soga, T., & Jimbo, T. *Mater. Lett.*, 2007, **61**, 3768.

[10] Wang, H., & Dai, H. *Chem. Soc. Rev.,* 2013, **42**, 3088.

[11] Badi, N., Erra, A. R., Hernandez, F. C. R., Okonkwo, A. O., Hobosyan, M., & Martirosyan, K. S. *Nanoscale Res. Lett.*, 2014, 9, 1.

[12] Wang, G. X., Yao, J., & Liu, H. K. *Electrochem. Solid ST.*, 2004, *7*, 250.

[13] Van de Vyver, S., Peng, L., Geboers, J., Schepers, H., de Clippel, F., Gommes, C. J., Goderis, B., Jacobs, P.A. & Sels, B. F. *Green chem.*, 2010, **12**, 1560.

[14] Liu, R., Shi, Y., Wan, Y., Meng, Y., Zhang, F., Gu, D., Chen, Z., Tu, B.& Zhao, D. *J. Am. Chem. Soc*., 2006, **128**, 11652.

[15] Bae, J. W., & Park, J. N. *Bull. Korean Chem. Soc.,* 2012, **33**, 3025.

[16] Wang, L., Gao, B., Peng, C., Peng, X., Fu, J., Chu, P. K., & Huo, K. *Nanoscale*, 2015, **7**, 13840.

[17] Lee, J. G., & Cutler, I. B. *Am. Ceram. Soc, Bull.*, 1975, **54**, 195.

[18] Chiew, Y. L., & Cheong, K. Y. *Mater. Sci. Eng. B*, 2011, **176**, 951.

[19] Piękos, R., & Paslawska, S. *Planta Medica*, 1976, **30**, 331.

[20]Krishnarao, R. V., Godkhindi, M. M., & Chakraborty, M. *Mater. Sci.,* 1992, **27**, 1227.

[21] Panigrahi, B. B., Roy, G. G., & Godkhindi, M. M. *Br. Ceram. Trans.,* 2001, **100**, 29.

[22] Desikachari TV, Cyanophyta, *Indian Council of Agricultural Research,* New Delhi,1959

[23] Krishnarao, R. V., Godkhindi, M. M., Mukunda, P. G. I., & Chakraborty, M. *J. Am. Ceram. Soc.,* 1991, **74**, 2869.

[24] Timothy, L. *Chem. Commun.,* 2007, **6**, 601.

[25] Chua, Y. T., Lin, C. X. C., Kleitz, F., & Smart, S. *J. Mater. Chem.*, 2015, **3**, 10480.

[26] Eletskii, P. M., Yakovlev, V. A., Kaichev, V. V., Yazykov, N. A., & Parmon, V. N. *Kinet. Catal.*, 2008,**49**, 305.

[27] Grill, A. *Annu Rev Mater Res.*, 2009, **39**, 49.

[28] Singh, L. P., Agarwal, S. K., Bhattacharyya, S. K., Sharma, U., & Ahalawat, S. *Nanomater. Nanotechno.,* 2011, **1**, 44.

[29] da Silva, J. G. E. *Carbon and Silicon Fluorescent Nanomaterials*, INTECH Open Access Publisher, Croatia, 2011.

[30] Erogbogbo, F., Tien, C. A., Chang, C. W., Yong, K. T., Law, W. C., Ding, H., Roy I, Swihart MT. & Prasad, P. N. *Bioconjugate. Chem.,* 2011, **22**, 1081.

[31] Zhang, L., Veerapandian, M., & Yun, K. S. *Bio. Chip. J.*, 2014, **8**, 83.

[32] Serpen, A., Capuano, E., Fogliano, V., Gokmen, V., *J. Agric. Food Chem.,* 2007, **55**, 7676.

[33] Deligiannakis, Y., Sotiriou, G. A., & Pratsinis, S. E. *ACS Appl. Mater. Inter.,* 2012, **4**, 6609.

[34] Shaji, J., & Varkey, D. *Int. J. Pharm. Investig.,* 2013, **43**, 405.

[35] Mukherjee, R., Borah, S. P., & Goswami, B. C. *J. Appl. Phycol*., 2010, **22**, 569.

[36] Begum, P. S., Joseph, R., Joseph, D., Kumar, P., & Ayswarya, E. P. *Int. J. Sci. Environ.Technol.*, 2013, **2**, 1027.